C-terminal peptides coassemble into Aβ42 oligomers and protect neurons against Aβ42-induced neurotoxicity

Erica A. Fradinger*†, Bernhard H. Monien*‡, Brigita Urbanc§¶, Aleksey Lomakin‖, Miao Tan**, Huiyuan Li*, Sean M. Spring*, Margaret M. Condron*, Luis Cruz§¶, Cui-Wei Xie**††, George B. Benedek‖‡‡§§, and Gal Bitan*††§§¶¶

Departments of *Neurology and **Psychiatry and Biobehavioral Sciences, David Geffen School of Medicine, ††Brain Research Institute, and ¶¶Molecular Biology Institute, University of California, Los Angeles, CA 90095; §Center for Polymer Studies, Department of Physics, Boston University, Boston, MA 02215; and ‖Center for Material Science and Engineering, Material Processing Center, and ‡‡Department of Physics, Massachusetts Institute of Technology, Cambridge, MA 02139

Contributed by George B. Benedek, July 23, 2008 (sent for review June 18, 2008)

Alzheimer's disease (AD) is an age-related disorder that threatens to become an epidemic as the world population ages. Neurotoxic oligomers of Aβ42 are believed to be the main cause of AD; therefore, disruption of Aβ oligomerization is a promising approach for developing therapeutics for AD. Formation of Aβ42 oligomers is mediated by intermolecular interactions in which the C terminus plays a central role. We hypothesized that peptides derived from the C terminus of Aβ42 may get incorporated into oligomers of Aβ42, disrupt their structure, and thereby inhibit their toxicity. We tested this hypothesis using Aβ fragments with the general formula Aβ(*x*−42) (*x* = 28–39). A cell viability screen identified Aβ(31–42) as the most potent inhibitor. In addition, the shortest peptide, Aβ(39–42), also had high activity. Both Aβ(31–42) and Aβ(39–42) inhibited Aβ-induced cell death and rescued disruption of synaptic activity by Aβ42 oligomers at micromolar concentrations. Biophysical characterization indicated that the action of these peptides likely involved stabilization of Aβ42 in nontoxic oligomers. Computer simulations suggested a mechanism by which the fragments coassembled with Aβ42 to form heterooligomers. Thus, Aβ(31–42) and Aβ(39–42) are leads for obtaining mechanism-based drugs for treatment of AD using a systematic structure–activity approach.

Alzheimer's disease | amyloid β-protein | inhibitor design

Alzheimer's disease (AD) is the predominant cause of dementia and one of the leading causes of death among elderly people. It is estimated that there are currently ≈27 million people suffering from AD worldwide (1). Because the world population is aging rapidly, if no cure is found in the near future AD will become an epidemic (2).

The amyloid cascade hypothesis proposed that amyloid β-protein (Aβ) fibrils—an aggregated form of Aβ found in amyloid plaques in the brains of patients with AD—were the neurotoxic agents causing AD (3). However, in recent years, multiple lines of evidence have led to a revision of this view, and today the primary toxins causing AD are believed to be early-forming Aβ oligomers rather than Aβ fibrils (4, 5). This paradigm shift suggests that efforts toward development of therapeutic agents targeting Aβ assembly should be directed at Aβ oligomers rather than fibrils. In particular, genetic, physiologic, and biochemical data indicate that oligomers of the 42-aa form of Aβ, Aβ42, are most strongly linked to the etiology of AD (6–9) and therefore are a particularly attractive target for inhibitor design.

Several groups have reported small-molecule inhibitors of Aβ oligomerization (10–13). The importance of understanding the mechanism of inhibition recently has been highlighted (14) after findings that many small-molecule inhibitors of fibrillogenesis may act nonspecifically, likely making them unsuitable for treating amyloid-related disorders (15). In addition, inhibition of fibril formation may actually lead to stabilization of toxic oligomers (16). Interestingly, when oligomers are stabilized by interaction with inhibitors or modulators, the toxicity of the resulting oligomers depends on the stabilizing molecule. For example, certain inositol derivatives, which were reported to inhibit Aβ-induced toxicity (17), presumably stabilize nontoxic Aβ oligomers (18). Nonetheless, to date, Aβ oligomerization inhibitors have been found empirically with limited mechanistic understanding of how they work, and currently mechanism-based inhibitor design targeting Aβ oligomerization is lacking.

A substantial body of work suggests that the C terminus of Aβ42 is a key region controlling Aβ42 oligomerization. Several studies of prefibrillar Aβ have suggested that the C terminus of Aβ42 is more rigid than the C terminus of the more abundant and less toxic Aβ40 (19–22). The increased rigidity has been attributed to interactions involving the C-terminal residues I41–A42, which stabilize a putative turn conformation (23). The higher conformational stability in the C terminus of Aβ42 correlates with formation oligomer populations distinct from those of Aβ40 (8, 23, 24) and with higher neurotoxicity (7, 9). Based on these data we hypothesized that molecules that possess high affinity for the C terminus of Aβ42 may disrupt oligomer formation and inhibit Aβ42-induced neurotoxicity. Because homotypic intermolecular interactions in the C terminus appear to be particularly important for Aβ42 self-assembly, we reasoned that peptides derived from this region might act as such inhibitors [supporting information (SI) Fig. S1]. We therefore prepared a series of Aβ42 C-terminal fragments (CTFs) (Table 1) and tested their capability of inhibiting Aβ42 toxicity and oligomerization.

Results

Solubility of CTFs. Being highly hydrophobic peptides, the CTFs were expected to be poorly soluble and to aggregate in aqueous solutions. To assess CTF solubility, peptide solutions were

Author contributions: E.A.F. and B.H.M. contributed equally to this work; E.A.F., B.H.M., B.U., and G.B. designed research; E.A.F., B.H.M., B.U., A.L., M.T., H.L., S.M.S., M.M.C., and G.B. performed research; L.C. contributed new reagents/analytic tools; E.A.F., B.H.M., B.U., A.L., M.T., H.L., S.M.S., C.-W.X., G.B.B., and G.B. analyzed data; and E.A.F., B.H.M., B.U., G.B.B., and G.B. wrote the paper.

The authors declare no conflict of interest.

†Present address: Department of Biology, Whittier College, 13406 East Philadelphia Street, Whittier, CA 90608.

‡Present address: Deutsches Institut für Ernährungsforschung Potsdam-Rehbrücke, Abt. Ernährungstoxikologie, Arthur-Scheunert-Allee 114–116, 14558 Nuthetal, Germany.

¶Present address: Department of Physics, Drexel University, Philadelphia, PA 19104.

§§To whom correspondence may be addressed. E-mail: benedek@mit.edu or gbitan@mednet.ucla.edu.

This article contains supporting information online at www.pnas.org/cgi/content/full/0807163105/DCSupplemental.

Table 1. Sequence and solubility of CTFs used in this study

CTF	Sequence	Solubility, μM
Aβ(28–42)	KGAIIGLMVGGVVIA	≈1
Aβ(29–42)	GAIIGLMVGGVVIA	22 ± 9
Aβ(30–42)	AIIGLMVGGVVIA	11 ± 3
Aβ(31–42)	IIGLMVGGVVIA	62 ± 18
Aβ(32–42)	IGLMVGGVVIA	52 ± 24
Aβ(33–42)	GLMVGGVVIA	134 ± 37
Aβ(34–42)	LMVGGVVIA	132 ± 29
Aβ(35–42)	MVGGVVIA	149 ± 33
Aβ(36–42)	VGGVVIA	134 ± 20
Aβ(37–42)	GGVVIA	143 ± 27
Aβ(38–42)	GVVIA	156 ± 33
Aβ(39–42)	VVIA	141 ± 30

The solubility values are average concentrations (±SE) measured by AAA for filtered solutions of each CTF in four to seven independent experiments.

prepared by initial dissolution in dilute NaOH (25), followed by dilution in phosphate buffer at physiologic pH and filtration through 20-nm cutoff filters. The concentration of each sample was then measured by amino acid analysis (AAA) (Table 1). CTFs up to 10 aa long could be dissolved at concentrations between 100 and 200 μM. Longer peptides had low solubility, but, except for Aβ(28–42), the solubility was sufficient for evaluation of neurotoxicity inhibition. Measurement of particle size by dynamic light scattering (DLS), β-sheet content by CD spectroscopy, and peptide morphology by EM indicated that, upon incubation in aqueous buffer at pH 7.4, CTFs longer than 5 aa aggregated at rates that ranged from a few hours to a few days depending on peptide length and sequence (data not shown). Direct comparison of aggregation rates was difficult because of the different solubility of the peptides.

Evaluation of CTF Toxicity. As peptides derived from Aβ42, the CTFs may have been neurotoxic themselves. To test for self-toxicity, CTFs were solubilized initially in DMSO and then diluted in cell culture medium. The solution was then centrifuged for 5 min at 16,000 × *g* to remove preformed large aggregates. The supernatant was added to differentiated PC-12 cells at the desired concentration. All of the solutions were clear to the eye when added to the cells, and the media remained clear at the end of the incubation period. Most of the CTFs showed no toxicity to neuronal cells up to the highest concentration used as assessed by the 3-(4,5-dimethylthiazol-2-yl)-2,5-diphenyltetrazolium bromide (MTT) cell-metabolism assay (26) (Fig. 1*A*), suggesting that they could be tested for inhibition of Aβ42-induced toxicity. An exception was Aβ(28–42), which was highly toxic (Fig. 1*A*), possibly because of the presence of K at the N terminus, which increases the positive charge at physiologic pH relative to the other CTFs.

Screening of CTFs for Inhibitory Activity. To evaluate the CTFs for inhibition of Aβ42-induced neurotoxicity, Aβ42 was dissolved in DMSO and diluted into cell culture medium. CTFs then were dissolved in DMSO and mixed with Aβ42 at an Aβ42:CTF concentration ratio of 1:10, respectively. The solution was centrifuged for 5 min at 16,000 × *g* to remove preformed aggregates and then added to differentiated PC-12 cells and incubated for 15 h. Cell viability was assessed by using the MTT assay.

All 12 CTFs were found to protect the cells to some degree from Aβ42-induced toxicity (Fig. 1*B*). Among them, Aβ(31–42) showed the highest inhibitory activity, fully rescuing the cells from Aβ42-induced toxicity. Aβ(39–42), the shortest CTFs used (only four amino acid residues), also showed high inhibitory activity (Fig. 1*B*). We therefore focus further discussion on these

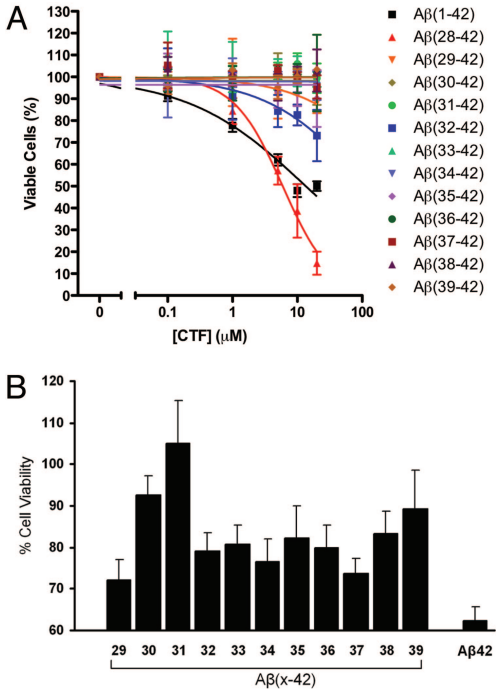

Fig. 1. Evaluation of CTF effect on neuronal cultures. CTFs at final nominal concentrations of 0.1–20 μM or mixtures of Aβ42:CTF at a 1:10 concentration ratio, respectively, were incubated with differentiated PC-12 cells. In *A*, Aβ42 (black squares) is shown for comparison. In *B*, the nominal concentration of Aβ42 is 5 μM. After 15 h of incubation, cell viability was measured by using the MTT assay. Cell culture medium containing DMSO in the same concentrations as used for peptide solubilization was used as a negative control, and 1 μM staurosporine was used as a positive control. The graphs show average data ± SD from at least three independent experiments, each performed with six wells per condition.

two peptides. Although Aβ(30–42) showed an activity level similar to that of Aβ(39–42), it was a less interesting peptide to study because it is structurally similar to, but less active than, Aβ(31–42).

Further Evaluation of Aβ(31–42) and Aβ(39–42) as Inhibitors of Aβ-Induced Neurotoxicity. To study the effectiveness of Aβ(31–42) and Aβ(39–42) as inhibitors of Aβ42-induced toxicity, dose dependence curves were generated. Aβ(31–42) and Aβ(39–42) yielded IC_{50} values of 14 ± 2 and 16 ± 5 μM in the MTT assay (Fig. S2*A*). The MTT assay measures cell metabolism rather than cell viability *per se*; however, because of the relatively short period required for this assay, it is a standard assay for investigations of Aβ toxicity (26, 27). In addition, Aβ(31–42) and Aβ(39–42) yielded IC_{50} values of 20 ± 4 and 47 ± 14 μM, respectively, in the lactate dehydrogenase (LDH) release assay (Fig. S2*B*), a direct measurement of cell death (28).

Synaptic failure has been postulated to be the primary event leading to the development of AD (5, 29). A decrease in the frequency of spontaneous miniature excitatory postsynaptic currents (mEPSCs) reflects a decline in the number of functional excitatory synapses or a reduction in presynaptic release probability. Aβ has been shown to inhibit synaptic function and decrease mEPSC frequency (30, 31). Here we used Aβ-induced attenuation of mEPSC frequency in primary mouse hippocampal neurons to evaluate the ability of Aβ(31–42) and Aβ(39–42) to rescue Aβ42-mediated synaptic toxicity.

Aβ42 and CTF mixtures were prepared in a manner similar to that used for cell viability assays, except that perfusion buffer (vehicle) was used instead of cell culture medium. After estab-

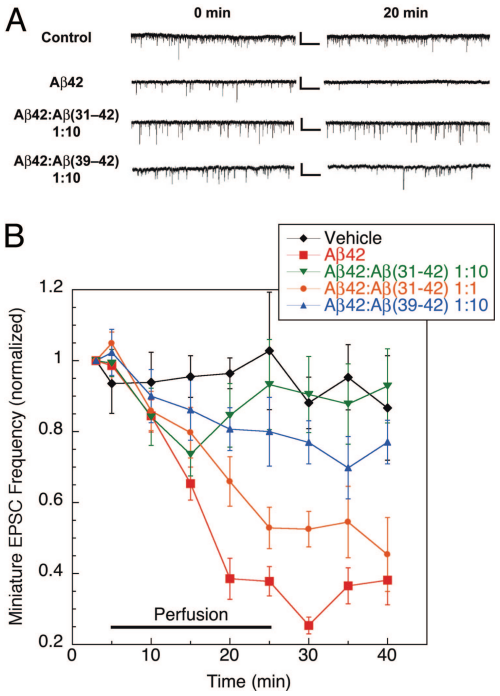

Fig. 2. CTFs rescue mEPSCs in Aβ42-treated hippocampal neurons. Mouse primary hippocampal neurons were exposed to vehicle ($n = 5$), 3 μM Aβ42 ($n = 8$), 1:1 Aβ42:Aβ(31–42) ($n = 9$), 1:10 Aβ42:Aβ(31–42) ($n = 10$), or 1:10 Aβ42:Aβ(39–42) ($n = 6$) mixtures, and the frequency and amplitude of mEPSCs were measured. (*A*) Representative recording traces collected before (0 min) and 20 min after peptide perfusion. Calibration bars: 25 pA/1 sec. (*B*) Cells were perfused with vehicle for 5 min to establish baseline, and then with peptide solutions for an additional 20 min, and allowed to recover in vehicle solution for 15 min. The curves show the time dependence of mEPSC frequency after exposure to Aβ42 in the absence or presence of CTFs over 40 min.

lishing a stable baseline recording for 5 min, cells were perfused with vehicle, Aβ42, or Aβ42:CTF mixtures at either 1:10 (both CTFs) or 1:1 [Aβ(31–42) only] concentration ratios, respectively, for 20 min, and washed for 15 min after perfusion. At 3 μM, Aβ42 was found to induce robust inhibition of mEPSCs, reducing spike frequency by 60–70% relative to baseline levels within 20 min (Fig. 2). This effect persisted after a 15-min washing period. Significant inhibition of the toxic effect of Aβ42 was observed at a 1:1 Aβ42:Aβ(31–42) concentration ratio, and at 10-fold excess Aβ(31–42) rescued mEPSC deficits completely (Fig. 2*B*), demonstrating that the CTF not only protected neuron viability, but also protected synaptic function from toxic insults by Aβ42 oligomers. Aβ(39–42) showed a somewhat lower, yet significant ($P < 0.05$), inhibitory effect at 10-fold excess relative to Aβ42 and was not studied at lower concentration ratios (Fig. 2). Changes in the amplitude of mEPSCs in the presence of Aβ42 or Aβ42:CTF mixtures relative to vehicle were not significant.

CTF Effect on Aβ42 Assembly. To gain insight into the mechanism by which CTFs inhibit Aβ42-induced toxicity we studied the interaction between the CTFs and Aβ42 during assembly using DLS, photo-induced cross-linking of unmodified proteins (PICUP), and discrete molecular dynamics (DMD), methods that have been useful for study of Aβ assembly (32–34).

For DLS experiments, mixtures of Aβ42:CTF at 30 μM nominal concentration each were prepared in 10 mM sodium phosphate (pH 7.4) and compared with Aβ42 alone. The actual concentration was determined *post facto* for each experiment by AAA. In the absence of CTFs, Aβ42 comprised predominantly particles with a hydrodynamic radius R_{H1} of ≈8–12 nm, which we designated as population 1 (P1, Fig. 3*A*, white bars). A minor population of larger particles, P2, with $R_{H2} \approx 20$–60 nm was observed in some, but not all, measurements. Both Aβ(31–42) and Aβ(39–42) induced substantial formation and accumulation of P2 particles (Fig. 3*A Top* and *Middle*, gray bars). In addition, Aβ(39–42) caused compaction of P1 particles to R_{H1} of ≈4–9 nm, whereas Aβ(31–42) did not. After 7 days of incubation in the absence of CTFs, Aβ42 formed particles of $R_H \approx 500$–1,000 nm (Fig. 3*A Bottom*, gray bars). Over a similar time period, slow growth of P2 up to an R_{H2} of ≈300 nm was observed in Aβ42:CTF mixtures. Quantitative analysis showed that the growth rate of P2 particles, dR_{H2}/dt, was decreased substantially in the presence of both CTFs relative to Aβ42 alone (Fig. 3*B*). It is important to note that, even though CTFs increase the abundance of P2 oligomers, the fraction of these oligomers is overrepresented in the DLS experiments because scattering from large particles is magnified proportionally to the square of their mass. Thus, P2 assemblies account for no more than a few percent of the total Aβ population.

In control DLS experiments using CTFs in the absence of full-length Aβ42 we observed a behavior different from the one described above. At 50 μM, Aβ(31–42) aggregated slowly, reaching particle size of ≈100 nm after several days. Distinct oligomer populations similar to P1 or P2 were not observed. Aβ(39–42) showed no aggregation at concentrations up to 140 μM.

As a complementary method for evaluating aggregation in Aβ42:CTF mixtures, we measured the average frequency of intensity spikes that occur when large particles, presumably fibrils, cross the DLS instrument's laser beam during the first 3 days of incubation (Fig. 3*C*). Both Aβ(31–42) and Aβ(39–42) showed substantial inhibition of fibril growth relative to Aβ42.

Next we investigated the effect of CTFs on formation of small oligomers using PICUP. When low-molecular-weight (LMW) Aβ42 (35) is subjected to PICUP and analyzed by SDS/PAGE, the most abundant oligomers observed are pentamers and hexamers, which self-assemble to form larger oligomers and therefore have been termed paranuclei (8). Paranucleus formation requires no incubation—these oligomers are observed immediately after dissolution and cross-linking of Aβ42. To study the effect of CTFs on these early-forming Aβ oligomers, ≈30 μM LMW Aβ42 was mixed with CTFs and cross-linked immediately. Importantly, the CTFs contain only residues that have little or no reactivity in PICUP chemistry (33). Therefore, cross-linking of CTFs to Aβ42 or to themselves was not observed, facilitating unhindered analysis of Aβ42 oligomer size distributions. Aβ(31–42) was found to cause a dose-dependent decrease in the formation of Aβ42 paranuclei at concentrations between ≈3 and 35 μM (Fig. S3) whereas Aβ(39–42) did not show this effect at a concentration as high as 155 μM (Fig. S3*B*). These data suggest that as the PICUP-inert Aβ(31–42) molecules coassemble with Aβ42, they spatially separate and "dilute" the Aβ42 monomers, preventing cross-linking. Aβ(39–42) might have induced a similar effect at a higher concentration if such high solubility could have been achieved. Alternatively, Aβ(39–42) may interfere with Aβ42-induced toxicity by a distinct mechanism that does not affect cross-linking.

Because of their noncrystalline and metastable nature, Aβ oligomers are not amenable to structural investigation using high-resolution experimental techniques, such as x-ray crystallography or solution-state NMR. To study the interactions between Aβ42 and CTFs during oligomerization in high resolution, we used computer simulations that combine DMD and a simplified protein structure. This approach, unlike traditional molecular dynamics using all-atom models, enables modeling of large molecular ensembles within relatively short times (34). Previously, this modeling strategy was used to study the oli-

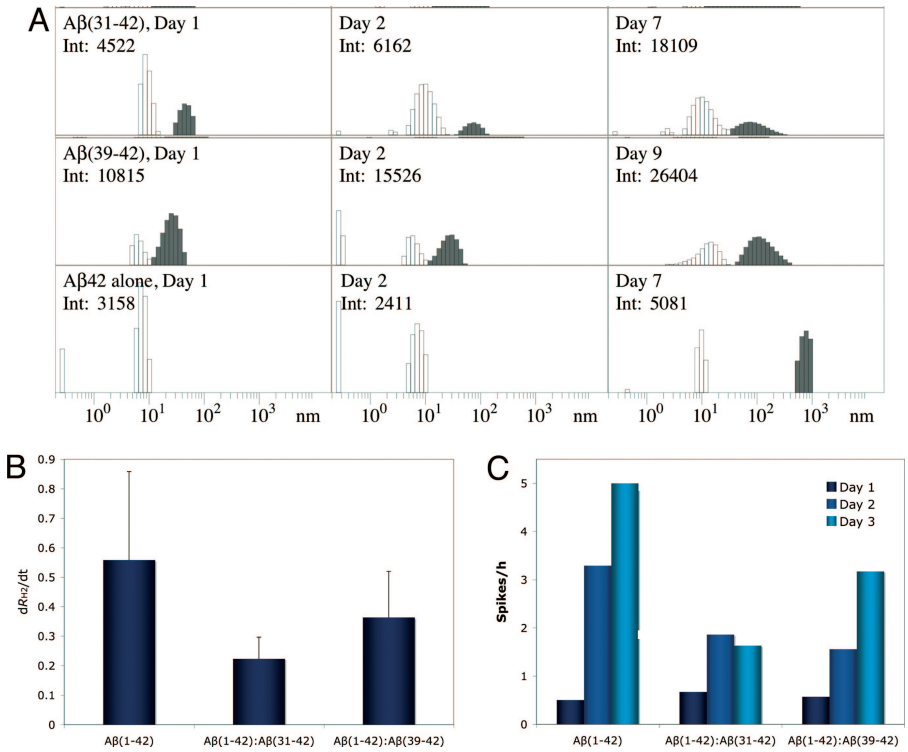

Fig. 3. CTF effect on Aβ42 assembly. (*A*) Representative distributions of Aβ42 in the absence or presence of CTFs immediately after preparation (*Left*), on the next day (*Center*), and after 7 or 9 days (*Right*). White bars represent P1 particles. Gray bars represent P2 or larger particles (in the case of Aβ42 alone). Days of measurement and the total scattering intensities in counts per second are shown in the upper left corner of each panel. Only intensities within the same row are directly comparable with each other. (*B*) Growth rates of P2 particles (dR_{H2}/dt) in the absence or presence of CTFs. (*C*) Average number of intensity spikes per hour during the first 3 days of measurement in the absence or presence of CTFs.

gomerization processes of Aβ40 and Aβ42 (23, 24), yielding oligomer size distributions in good agreement with experimental findings (8, 36).

Here we modeled the self-assembly of Aβ42 in the presence of Aβ(31–42) or Aβ(39–42), each at Aβ42:CTF number concentration ratios ranging from 1:1 to 1:8. In all cases, we found that Aβ42 and the CTF molecules coassembled into "heterooligomers." An example is shown in Fig. 4*A*. Formation of heterooligomers of Aβ42 and Aβ(31–42) was observed already after 10^5 simulation steps, and by 10^7 steps all of the molecules associated into one large heterooligomer. Movie S1 shows the time evolution of the heterooligomers. This behavior was observed for the Aβ42:Aβ(31–42) system at 1:2 and higher ratios, whereas in the Aβ42:Aβ(39–42) system a 1:8 ratio was necessary for the coassembly of all of the molecules into one heterooligomer. Within the heterooligomers, intermolecular interactions among Aβ42 monomers were inhibited. Aβ(31–42) was found to inhibit these intermolecular interactions substantially more efficiently than Aβ(39–42) (Fig. 4*B*).

Discussion

We have used an approach for developing Aβ42 oligomerization inhibitors based on putative homotypic association of peptide sequences in the C terminus of Aβ42. Peptides derived from the C terminus of Aβ42 were found to disrupt the assembly and inhibit the neurotoxicity of Aβ42 oligomers. This proof-of-concept study using Aβ42 CTFs has yielded two lead peptide inhibitors of Aβ42 assembly and neurotoxicity, Aβ(31–42) and Aβ(39–42). The higher inhibitory activity of Aβ(31–42) and Aβ(39–42) relative to other CTFs suggests that the inhibition is specific rather than based on generic hydrophobic association.

In our initial screen, in which Aβ42 was mixed with each CTF at a 1:10 ratio, respectively, Aβ(31–42) was the only CTF that completely rescued the cells from Aβ42-induced toxicity. It was followed by Aβ(30–42) and Aβ(39–42), each of which attenuated Aβ42 toxicity by ≈80% (Fig. 1*B*). When the inhibitory activity is plotted versus CTF length, Aβ(31–42) gives rise to an inhibitory activity peak (Fig. 1*B*). The high activity of Aβ(30–42) was interpreted as resulting from its close similarity to Aβ(31–42). In contrast, the high activity of Aβ(39–42) was surprising given its small size and presumed absence of stable conformation.

In the three biological tests applied, cell death (LDH assay), mitochondrial integrity (MTT assay), and synaptic function (mEPSC assay), Aβ(31–42) consistently showed higher potency as an inhibitor of Aβ42-induced toxicity than Aβ(39–42). Structural studies of Aβ42 have suggested the existence of a quasi-stable conformation in the C terminus (19–22), likely a turn centered at G37–G38 (23, 24, 37). We conjecture that this conformation is important for intermolecular interaction among the C termini of Aβ42 that lead to oligomerization. A similar putative structure in Aβ(31–42) may account, at least partially, for the high inhibitory activity of this peptide. In contrast, Aβ(39–42) is not expected to have a stable conformation. These considerations, and the fact that Aβ(31–42) is three times as long as Aβ(39–42), suggest that the two CTFs may act by different mechanisms.

We anticipated that CTFs would disrupt Aβ42 oligomerization by incorporating into a putative hydrophobic core of Aβ42 oligomers (Fig. S1), in which the C terminus was predicted to be an important component. Our physicochemical studies suggest that the CTFs indeed interact with Aβ42 molecules and get incorporated into oligomers. DLS data (Fig. 3*A*) show two initial oligomeric populations of Aβ42, high-abundance, small oli-

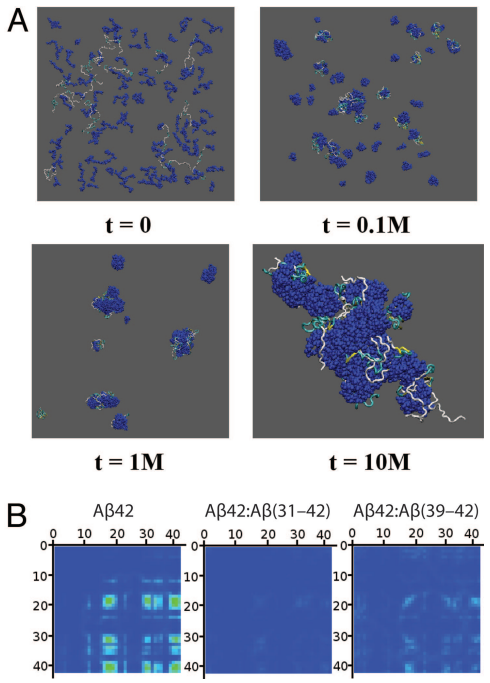

Fig. 4. Simulation of the interaction between Aβ42 and CTFs during oligomerization. (*A*) Configurations of 16 Aβ42 and 128 Aβ(31–42) molecules at different time frames measured at *t* simulation steps. CTFs are displayed in dark blue, and Aβ42 molecules are represented by their secondary structure: yellow ribbons, β-strands; blue tubes, turns; silver tubes, random coil. (*B*) Intermolecular contact maps of Aβ42 in the absence or presence of CTFs calculated for the highest Aβ42:CTF peptide number concentration ratio (1:8). The contact maps are oriented such that the contact strength between pairs of N-terminal residues is displayed at the top left corner and the contact strength between pairs of C-terminal residues is at the bottom right corner. The strength of the contact between two amino acids is color-coded from 0.0 (blue) to a maximal strength (red), corresponding to 30 contacts.

gomers of $R_H \approx 8$–12 nm (P1) and low-abundance, intermediate-size oligomers of $R_H \approx 20$–60 nm (P2). In the presence of Aβ(31–42) and Aβ(39–42), P2 oligomers are stabilized and their growth is attenuated (Fig. 3 *A* and *B*). In addition, both CTFs inhibit formation of intensity spikes in DLS experiments (Fig. 3*C*), suggesting inhibition of fibril formation. In correlation with the higher inhibitory activity observed for Aβ(31–42) in the MTT, LDH, and mEPSC assays, it was found to inhibit both the increase in size of P2 particles and the average number of intensity spikes per hour with higher potency than Aβ(39–42) (Fig. 3 *B* and *C*). In addition, CTFs that showed low inhibition of toxicity had little effect on particle growth (data not shown), demonstrating an overall good agreement between inhibition of particle growth and inhibition of toxicity.

In support of different mechanisms of toxicity inhibition by Aβ(31–42) and Aβ(39–42), only Aβ(39–42) was found to reduce the size of the P1 oligomer population to ≈4–9 nm, suggesting that interaction with Aβ(39–42) altered the tertiary and/or quaternary structure of Aβ42 within P1 oligomers. Another important difference between the two CTFs was found in PICUP experiments, in which Aβ(31–42) was found to inhibit paranucleus formation dose-dependently (Fig. S3), whereas Aβ(39–42) did not show such inhibition at the highest concentration tested (Fig. S3*B*).

The observed differences between the behaviors of Aβ(31–42) and Aβ(39–42) in both the PICUP and the DLS experiments correlated qualitatively with the simulation findings. In agreement with the PICUP data, the model predicted more efficient disruption of intermolecular contacts among Aβ42 monomers by Aβ(31–42) than by Aβ(39–42) (Fig. 4*B*). The computer simulations also help explaining, qualitatively, how CTFs can both disrupt paranucleus formation and promote formation of P2 oligomers. In the model, relatively large heterooligomers are observed at high numbers of simulation steps (Fig. 4*A*). Interruption of intermolecular contacts within these heterooligomers by CTFs suggests that their cross-linking by PICUP would be inhibited because the cross-linking is "zero length"; i.e., it requires direct intermolecular interactions between Aβ42 monomers.

Taken together, the data indicate that the CTFs inhibit Aβ42-induced toxicity by formation of nontoxic heterooligomers, similar to the mechanism proposed for the inhibitory activity of inositols (17, 18) and for the green tea-derived polyphenol epigallocatechin gallate (38). The observation that highly hydrophobic peptides are acting by a mechanism similar to that of polyols is interesting and suggests that stabilization of nontoxic oligomers may be a general mechanism for compounds that inhibit the toxic effects of amyloidogenic proteins. Using peptides derived from the C terminus of Aβ42, rather than carbohydrate-based inhibitors, allows delineating the relationship between inhibitor structure and bioactivity, providing a framework for development of future derivatives. An advantage of using CTFs as inhibitors is that the hydrophobic nature of these peptides may facilitate penetration through biological barriers, such as the plasma membrane and the blood–brain barrier. Our findings provide a foundation for lead optimization by systematic structure–activity relationship studies. Aβ(31–42) is a potent inhibitor of toxicity that may be optimized by using standard methods, such as alanine scanning and introduction on nonnatural amino acids. Aβ(39–42) is a somewhat weaker inhibitor, but its small size may facilitate transformation into peptidomimetics leading to novel, disease-modifying drugs for AD.

Methods

Peptide Preparation. Aβ42 and CTFs were synthesized by Fmoc chemistry using automated Applied Biosystems 433A synthesizers, purified, and characterized by AAA and mass spectrometry as described previously (39, 40). For additional details, see *SI Text*.

Cell Culture. Rat pheochromocytoma (PC-12) cells were used 48 h after differentiation. Primary embryonic hippocampal cultures were maintained for 2 weeks before initiation of experiments. For additional details, see *SI Text*.

Cell Viability Assays. The biological activity of the CTFs themselves and of Aβ42:CTF mixtures was assessed by the CellTiter 96 Cell Proliferation Assay (MTT assay; Promega) and CytoTox-ONE Homogenous Membrane Integrity Assay (LDH assay; Promega). For additional details, see *SI Text*.

Electrophysiological Studies. Spontaneous mEPSCs were recorded at a holding potential of −70 mV by using an Axopatch 200A patch-clamp amplifier (Axon Instruments). For additional details, see *SI Text*.

DLS. Aβ42:CTF mixtures prepared at 30 μM (nominal concentration) of each peptide were studied by using an in-house-built system with a He-Ne laser model 127 (wavelength 633 nm, power 50 mW; Coherent) as a light source. For additional details, see *SI Text*.

PICUP. Aβ42:CTF mixtures were prepared in 10 mM sodium phosphate (pH 7.4) and subjected immediately to PICUP as described previously (33). For additional details, see *SI Text*.

DMD. DMD simulations were performed by using a four-bead protein model with backbone hydrogen bonding and effective amino acid-specific interactions due to hydropathy, as described previously (23, 24). For additional details, see *SI Text*.

ACKNOWLEDGMENTS. We express our gratitude for financial support from National Institutes of Health/National Institute on Aging Grants AG027818 and AG023661, Grant 2005/2E from the Larry L. Hillblom Foundation, a private donation from Mr. Stephen Bechtel, Jr., and a generous gift from the Turken family.

1. Brookmeyer R, Johnson E, Ziegler-Graham K, Arrighi HM (2007) Forecasting the global burden of Alzheimer's disease. *Alzheimer's Dementia* 3:186–191.
2. Alzheimer Association (2008) 2008 Alzheimer's disease facts and figures. *Alzheimer's Dementia* 4:110–133.
3. Hardy JA, Higgins GA (1992) Alzheimer's disease: The amyloid cascade hypothesis. *Science* 256:184–185.
4. Kirkitadze MD, Bitan G, Teplow DB (2002) Paradigm shifts in Alzheimer's disease and other neurodegenerative disorders: The emerging role of oligomeric assemblies. *J Neurosci Res* 69:567–577.
5. Walsh DM, Selkoe DJ (2007) Aβ oligomers—A decade of discovery. *J Neurochem* 101:1172–1184.
6. Borchelt DR, *et al.* (1996) Familial Alzheimer's disease-linked presenilin 1 variants elevate Aβ1–42/1–40 ratio in vitro and in vivo. *Neuron* 17:1005–1013.
7. Dahlgren KN, *et al.* (2002) Oligomeric and fibrillar species of amyloid-β peptides differentially affect neuronal viability. *J Biol Chem* 277:32046–32053.
8. Bitan G, *et al.* (2003) Amyloid β-protein (Aβ) assembly: Aβ40 and Aβ42 oligomerize through distinct pathways. *Proc Natl Acad Sci USA* 100:330–335.
9. McGowan E, *et al.* (2005) Aβ42 is essential for parenchymal and vascular amyloid deposition in mice. *Neuron* 47:191–199.
10. Wang Z, Chang L, Klein WL, Thatcher GR, Venton DL (2004) Per-6-substituted-per-6-deoxy β-cyclodextrins inhibit the formation of β-amyloid peptide derived soluble oligomers. *J Med Chem* 47:3329–3333.
11. Walsh DM, *et al.* (2005) Certain inhibitors of synthetic amyloid β-peptide (Aβ) fibrillogenesis block oligomerization of natural Aβ and thereby rescue long-term potentiation. *J Neurosci* 25:2455–2462.
12. Yang F, *et al.* (2005) Curcumin inhibits formation of amyloid β oligomers and fibrils, binds plaques, and reduces amyloid in vivo. *J Biol Chem* 280:5892–5901.
13. Necula M, Kayed R, Milton S, Glabe CG (2007) Small molecule inhibitors of aggregation indicate that amyloid β oligomerization and fibrillization pathways are independent and distinct. *J Biol Chem* 282:10311–10324.
14. Research Highlights (2008) Chemical biology: Aggravating aggregating. *Nature* 451:608–609.
15. Feng BY, *et al.* (2008) Small-molecule aggregates inhibit amyloid polymerization. *Nat Chem Biol* 4:197–199.
16. Martins IC, *et al.* (2008) Lipids revert inert Aβ amyloid fibrils to neurotoxic protofibrils that affect learning in mice. *EMBO J* 27:224–233.
17. McLaurin J, *et al.* (2006) Cyclohexanehexol inhibitors of Aβ aggregation prevent and reverse Alzheimer phenotype in a mouse model. *Nat Med* 12:801–808.
18. McLaurin J, Golomb R, Jurewicz A, Antel JP, Fraser PE (2000) Inositol stereoisomers stabilize an oligomeric aggregate of Alzheimer amyloid β peptide and inhibit Aβ-induced toxicity. *J Biol Chem* 275:18495–18502.
19. Murakami K, *et al.* (2005) Formation and stabilization model of the 42-mer Aβ radical: Implications for the long-lasting oxidative stress in Alzheimer's disease. *J Am Chem Soc* 127:15168–15174.
20. Riek R, Guntert P, Döbeli H, Wipf B, Wüthrich K (2001) NMR studies in aqueous solution fail to identify significant conformational differences between the monomeric forms of two Alzheimer peptides with widely different plaque-competence, Aβ(1–40)^{ox} and Aβ(1–42)^{ox}. *Eur J Biochem* 268:5930–5936.
21. Sgourakis NG, Yan Y, McCallum SA, Wang C, Garcia AE (2007) The Alzheimer's peptides Aβ40 and 42 adopt distinct conformations in water: A combined MD/NMR study. *J Mol Biol* 368:1448–1457.
22. Lazo ND, Grant MA, Condron MC, Rigby AC, Teplow DB (2005) On the nucleation of amyloid β-protein monomer folding. *Protein Sci* 14:1581–1596.
23. Urbanc B, *et al.* (2004) *In silico* study of amyloid β-protein folding and oligomerization. *Proc Natl Acad Sci USA* 101:17345–17350.
24. Yun S, *et al.* (2007) Role of electrostatic interactions in amyloid β-protein (Aβ) oligomer formation: A discrete molecular dynamics study. *Biophys J* 92:4064–4077.
25. Fezoui Y, *et al.* (2000) An improved method of preparing the amyloid β-protein for fibrillogenesis and neurotoxicity experiments. *Amyloid* 7:166–178.
26. Datki Z, *et al.* (2003) Method for measuring neurotoxicity of aggregating polypeptides with the MTT assay on differentiated neuroblastoma cells. *Brain Res Bull* 62:223–229.
27. Shearman MS, Ragan CI, Iversen LL (1994) Inhibition of PC12 cell redox activity is a specific, early indicator of the mechanism of β-amyloid-mediated cell death. *Proc Natl Acad Sci USA* 91:1470–1474.
28. Korzeniewski C, Callewaert DM (1983) An enzyme-release assay for natural cytotoxicity. *J Immunol Methods* 64:313–320.
29. Haass C, Selkoe DJ (2007) Soluble protein oligomers in neurodegeneration: Lessons from the Alzheimer's amyloid β-peptide. *Nat Rev Mol Cell Biol* 8:101–112.
30. Chin JH, Ma L, MacTavish D, Jhamandas JH (2007) Amyloid β protein modulates glutamate-mediated neurotransmission in the rat basal forebrain: Involvement of presynaptic neuronal nicotinic acetylcholine and metabotropic glutamate receptors. *J Neurosci* 27:9262–9269.
31. Parameshwaran K, *et al.* (2007) Amyloid β-peptide Aβ(1–42) but not Aβ(1–40) attenuates synaptic AMPA receptor function. *Synapse* 61:367–374.
32. Lomakin A, Teplow DB (2006) Quasielastic light scattering study of amyloid β-protein fibril formation. *Protein Pept Lett* 13:247–254.
33. Bitan G (2006) Structural study of metastable amyloidogenic protein oligomers by photo-induced cross-linking of unmodified proteins. *Methods Enzymol* 413:217–236.
34. Urbanc B, Borreguero JM, Cruz L, Stanley HE (2006) Ab initio discrete molecular dynamics approach to protein folding and aggregation. *Methods Enzymol* 412:314–338.
35. Bitan G, Teplow DB (2005) Preparation of aggregate-free, low molecular weight amyloid-β for assembly and toxicity assays. *Methods Mol Biol* 299:3–9.
36. Bernstein SL, *et al.* (2005) Amyloid β-protein: Monomer structure and early aggregation states of Aβ42 and its Pro19 alloform. *J Am Chem Soc* 127:2075–2084.
37. Takano K, *et al.* (2006) Structure of amyloid β fragments in aqueous environments. *FEBS J* 273:150–158.
38. Ehrnhoefer DE, *et al.* (2008) EGCG redirects amyloidogenic polypeptides into unstructured, off-pathway oligomers. *Nat Struct Mol Biol* 15:558–566.
39. Lomakin A, Chung DS, Benedek GB, Kirschner DA, Teplow DB (1996) On the nucleation and growth of amyloid β-protein fibrils: Detection of nuclei and quantitation of rate constants. *Proc Natl Acad Sci USA* 93:1125–1129.
40. Condron MM, Monien BH, Bitan G (2008) Synthesis and purification of highly hydrophobic peptides derived from the C-terminus of amyloid β-protein. *Open Biotechnol J* 2:87–93.